Colloids and Surfaces A: Physicochem. Eng. Aspects 455 (2014) 49–57

Contents lists available at ScienceDirect

Colloids and Surfaces A: Physicochemical and Engineering Aspects

journal homepage: www.elsevier.com/locate/colsurfa

An insight into the surface properties of calcined kaolinitic clays: The grinding effect

J.A.F. Gamelas[a,*], E. Ferraz[b], F. Rocha[c]

[a] Department of Chemical Engineering, CIEPQPF, University of Coimbra, Pólo II. R. Sílvio Lima, PT - 3030-790 Coimbra, Portugal
[b] Polytechnic Institute of Tomar, GeoBioTec Research Unit, Quinta do Contador, Estrada da Serra, PT - 2300-313 Tomar, Portugal
[c] Geosciences Department, GeoBioTec Research Unit, University of Aveiro, Campus Universitário de Santiago, PT- 3810-193 Aveiro, Portugal

HIGHLIGHTS

- Surface Lewis basic properties increase from kaoline to metakaolinitic materials.
- The extensive grinding of metakaolinitic materials affords a decrease of the γ_s^d.
- Lewis basic properties of the metakaolines surface also increase with grinding.
- Grinding results are largely explained by changes in the surface nanoroughness.
- Shown results may have interest in the composites area/cation-exchange properties.

GRAPHICAL ABSTRACT

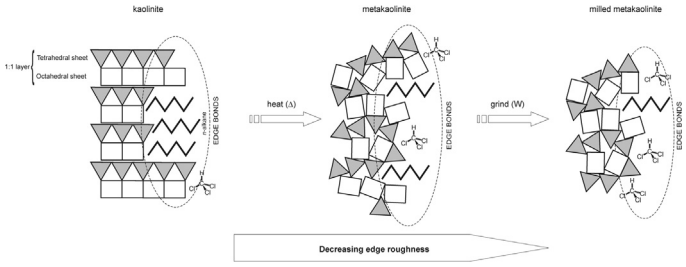

ARTICLE INFO

Article history:
Received 11 February 2014
Received in revised form 7 April 2014
Accepted 10 April 2014
Available online 24 April 2014

Keywords:
Calcined kaolins
Metakaolins
IGC
XPS
Adsorption
Grinding

ABSTRACT

The present work aimed characterizing in a systematic way the surface of metakaolinitic materials produced by calcination of a kaolinitic clay at different temperatures and to study the effect of grinding on the surface properties of metakaolinitic materials. Using X-ray photoelectron spectroscopy, it was found for all materials a Si/Al atomic ratio close to 1, confirming the presence of the 1:1 clay structure. By inverse gas chromatography, an increase of the Lewis basic properties of the surfaces of metakaolinitic materials in comparison to the original clay was found, which was due to the condensation of hydroxyl groups in the structure of the clay. The grinding of the metakaolinitic materials afforded a decrease of the dispersive component of the surface energy (γ_s^d) as well as an increase of the specific interaction with sterically hindered molecules, caused by the diminishing of the materials surface nanoroughness. The Lewis basic properties of the materials surface also increased with grinding. Noticeably, for all studied materials a good inverse relation could be found between the γ_s^d and the specific interaction of trichloromethane (but not with dichloromethane), showing the importance of surface nanoroughness on the adsorption process of bulky molecules.

1. Introduction

Calcined kaolin or metakaolin is an artificial material used in advanced ceramics [1,2], as filler in papermaking, [3,4], as a pozzolanic material in mortars [5,6], concrete [7,8] and cement-wood composites [9], as extender in plastics [10] and natural rubber

* Corresponding author.
E-mail addresses: jafgas@eq.uc.pt, jose.antonio@ua.pt (J.A.F. Gamelas).

http://dx.doi.org/10.1016/j.colsurfa.2014.04.038
0927-7757/

[11], as opacifier in oral medicine prosthesis [12], in processing of oil shale [13] and food wastes [7], in paints [14], and as a fundamental component for the production of some types of inorganic polymeric materials – geopolymers [2,15]. Metakaolin contains high content of Si and Al and is obtained by heating (calcinating) kaolin raw material, a georesource mainly composed by kaolinite, [$Al_2Si_2O_5(OH)_4$)]. The calcination process at temperatures ranging from ≈450 °C to ≈750 °C promotes the removal of the structural water (dehydroxylation) in kaolinite and its transformation into metakaolinite that is an amorphous (disordered) aluminosilicate. Calcination at higher temperature (>950 °C) results in the formation of crystalline phases, such as silicon-spinel or mullite.

The physico-chemical surface properties of calcined clays have high importance considering their influence in the context of the production of composites with polymeric matrices (e.g., composites with cellulose for papermaking, when calcined materials are used as fillers), or in cation exchange processes or pozzolanic reactions.

Inverse gas chromatography (IGC) is a suitable technique to assess the surface properties of fibrous materials (e.g., glass fibres and cellulosic fibres) and powders such as clays and calcined clays since it gives a wide range of physico-chemical surface parameters not accessed by other techniques. On this point, contact angle measurements are not so adequate for the analysis of powders due to the associated problems of heterogeneity, roughness, porosity, and surface energy gradients. Another useful technique to study the materials surface is the X-ray photoelectron spectroscopy (XPS) that can provide information of the chemical composition and structure of the surface up to about 10 nm depth.

Several studies have been reported on the use of IGC to evaluate the surface properties on clayey materials, such as kaolinites [16–22], illites [16,17,22], smectites [23,24], and palygorskites (attapulgites) [25,26]. In particular, the dispersive component of the surface energy and the surface morphology of kaolinites (and illites) were evaluated by IGC using *n*-alkanes and branched alkanes as probes [16]. For the same type of materials, the effect of pre-conditioning temperature on the heats of adsorption of several organic probes was also considered [22]. Regarding calcined kaolinitic clays, Burry and Keller [18] analysed the effect of the pre-conditioning temperature on the dispersive component of the surface energy (at 100 °C) of two calcined clays (one experimental and another commercial) and compared with kaolin samples. Ansari and Price [27] analysed two commercial grades of calcined kaolin for their dispersive properties and specific interactions with a few probes, in order to produce composites with polyethylene. These two pioneer studies were restricted to a small number of calcined clays and the specific acid-base interactions were not in depth analysed. On the other hand, the use of XPS on calcined kaolinitic materials has also been reported (e.g. [28]).

In the present study, one kaolinitic raw material as starting material, five experimental metakaolins and one commercial metakaolin were thoroughly analysed by IGC and XPS in order to evaluate the surface properties of these materials. Several methods for the IGC data analysis were employed, in order to obtain a wide range of parameters of the surface properties of the calcined kaolinitic materials. Particular emphasis was given to the grinding effect on the surface properties of calcined kaolinitic clays.

2. Materials and methods

2.1. Materials

A kaolinitic raw material (kaolinitic mud) collected from an industrial sand wash plant was the starting material used in this study. The kaolinitic raw material was calcined in an oxidizing atmosphere, on a 2.5 m scale prototype rotary kiln with fast firing cycles (1:00 h to 1:30 h), in order to obtain experimental metakaolinized samples. Three experimental calcined kaolinitic clays (referenced as "MK") were obtained after calcination of the kaolinitic raw material at 750 °C, 840 °C and 940 °C. After the calcination, the materials were subjected to a disaggregation stage in an alumina ball mill (Gabbrielli Fast Mill) during 5 min. Two experimental metakaolinized samples were also subjected to an additional grinding (milling) stage (referenced as "M"), which was accomplished in a vibratory agate disc mill (Retsch RS1) during 20 min at 700 rpm. The experimental metakaolinized samples were compared with the commercial Optipozz (Burgess, USA) highly-reactive metakaolin, which served as reference to the parameters evaluated in this study. Overall, six samples of metakaolins (MK-750, MK-840, MK-940, MK-750-M, MK-940-M, MK-USA) and the sample of the initial kaolinitic raw material (referenced as "K") were considered for analyses.

2.2. Methods

The materials were analysed for their mineralogical composition, particle size and specific surface area. The mineralogical analysis was performed by powder X-ray diffraction (XRD) in a Philips X'Pert PRO MPD diffractometer. The crystalline phases were identified by comparison with the standards from the International Centre for Diffraction Data. Particle size analysis was carried out by sedimentation and absorption of X-rays in a Micromeritics Sedigraph 5100 apparatus. The determination was performed in the 0.1–63 μm size range. Specific surface area was determined by N_2 adsorption in a Micromeritics Gemini 2.0 instrument, using the BET method. Samples were pre-treated at 200 °C under a nitrogen flow before measurements were made.

2.3. Inverse gas chromatography and X-ray photoelectron spectroscopy

The clayey materials were analysed by inverse gas chromatography and X-ray photoelectron spectroscopy, in order to assess their surface properties and surface chemical composition.

The material for IGC analysis was previously compacted through axial compression of 6–7 g of powder at ≈120 MPa. The pressed disc was then crumbled in a porcelain mortar and finally sieved between 710 and 500 μm to obtain "coarse" granulates, before being packed in the IGC column. Using this procedure it was possible to obtain enough gas flow rate in the IGC column. IGC analysis was done using a DANI GC 1000 digital pressure control gas chromatograph equipped with a hydrogen flame ionization detector. Stainless-steel columns, 0.5 m long and 0.4 cm inner diameter were washed with acetone and dried before packing. Approximately 5 g of each sample was packed into the gas chromatograph column. The columns were shaped in a smooth "U" to fit the detector/injector geometry of the instrument. The packed columns were conditioned overnight at 110 °C, under a helium flow, before any measurements were made. Experiments were carried out at a column temperature of 110 °C with the injector and detector kept at 180 °C and 200 °C, respectively. Helium was used as carrier gas with flow rates typically between 25 and 40 mL/min. Small quantities of probe vapor (<1 μl) were injected into the carrier gas, allowing work under infinite dilution conditions. The probes used for the IGC data collection were *n*-pentane (C5), *n*-hexane (C6), *n*-heptane (C7), *n*-octane (C8), trichloromethane (TCM), dichloromethane (DCM), 1-pentene, 1-hexene, and cyclohexane (CyHex). All probes were of chromatographic grade and were used as received (Sigma–Aldrich). Methane was used as the reference probe. The retention times (t_r) were the average of three

injections and were determined by the Conder and Young method [29]. Ethyl ether, tetrahydrofurane, acetone and ethyl acetate were also tested but could not be measured (no elution was detected) due to strong interaction of these probes with the analysed materials..

The X-ray photoelectron spectra were obtained using a Kratos AXIS Ultra HSA equipment. The analysis was carried out with a monochromatic Al Kα X-ray source (1486.7 eV), operating at 15 kV (90 W), in fixed analyser transmission mode, with a pass energy of 80 eV. Wide scan survey spectra were recorded at take-off angle of 90° and between 0 eV and 1350 eV binding energy with a step size of 1 eV and dwell time of 200 ms. Data acquisition, with VISION software, was performed at an ultra-vacuum pressure (<1.0E−6 Pa), and a charge neutralisation system was used. Quantitative data analysis was done using the following atomic sensitivity factors: Si = 0.328; Al = 0.193; O = 0.78; C = 0.278; N = 0.477; Mg = 2.62; K = 1.47; Fe = 2.96; F = 1; Ti = 2). All spectra were corrected for charging effects with respect to adventitious hydrocarbon C 1s peak. The relative atomic quantification (normalized to 100%) was done with 3 scans carried out in 3 different survey areas. Pellets of about 1 cm diameter and 1 mm thickness were prepared for the analysis by pressing the samples at ≈20 MPa during 3 min.

2.4. IGC theoretical background

The principles and mathematical formalism of inverse gas chromatography have been widely described by several authors [30–32]. Briefly, the retention of a gas or vapour probe molecule in the IGC column is quantified by the net retention volume, V_n, which is the volume of inert carrier gas that is necessary to push the probe molecule through the chromatographic column containing the solid sample under analysis. V_n can be calculated from IGC data using Eq. (1), where t_r is the retention time of the injected probe through the column, t_0 is the retention time of the non-interacting probe (methane), F is the corrected flow rate of the inert carrier gas and J is the James–Martin correction factor for the carrier gas compressibility.

$$V_n = (t_r - t_0)FJ \tag{1}$$

At infinite dilution conditions, where probe-probe interactions are negligible and V_n depends only on the sample–probe interactions, the free energy of adsorption of the probe on the stationary phase surface, per mole, ΔG_a, can be determined from the retention volume, V_n, according to Eq. (2). In this equation, R is the gas constant, T is the absolute column temperature and K is a constant dependent on the chosen reference state [30,33].

$$\Delta G_a = -RT\ln(V_n) + K \tag{2}$$

If only dispersive interactions occur between sample and probe, the net retention volume, V_n, can be related to the dispersive components of the surface free energy of the interacting solid and probe, γ_s^d and γ_l^d, respectively, by Eq. (3), where N is the Avogadro number and a is the molecular surface area of the probe. According to Eq. (3), the dispersive component of the surface energy of the analysed sample may be estimated from the slope of the linear fit of $RT\ln(V_n)$ as a function of $2Na(\gamma_l^d)^{0.5}$, using the IGC data obtained with the apolar probes (Schultz and Lavielle approach) [34].

$$RT\ln(V_n) = \sqrt{\gamma_s^d}\,2Na\sqrt{\gamma_l^d} + K \tag{3}$$

Other methods are available for the determination of γ_s^d. In the Dorris and Gray approach [33] the dispersive component of the surface energy (γ_s^d) is determined from the difference in the free energy of adsorption due to the introduction of an additional –CH_2– group into the carbon chain of a n-alkane probe (Eq. (4)). a_{CH_2} is the molecular area of the –CH_2– group, which is usually taken as 0.06 nm^2 and γ_{CH_2} is the surface energy of a solid entirely composed of methylene groups (Eq. 5) [30,33]. The drawbacks and advantages of each approach used to calculate γ_s^d have been thoroughly discussed in the literature [31].

$$\gamma_s^d = \frac{\left[RT\ln(V_n^{(C_{n+1}H_{2n+4})}/V_n^{(C_nH_{2n+2})})\right]^2}{4N^2(a_{CH_2})^2\gamma_{CH_2}} \tag{4}$$

$$\gamma_{CH_2} = 35.6 + 0.058(293.15 - T) \tag{5}$$

For the polar probes, there is a corresponding specific component contribution, ΔG_a^s, in addition to the dispersive component, to the overall free energy of adsorption [30]. This parameter (ΔG_a^s) can be estimated by calculating the difference between the experimental value of $RT\ln(V_n)$ obtained for the polar probe and the corresponding estimation for the reference apolar probe (Eq. (6)) based on the linear fitting of $RT\ln(V_n)$ vs. $2Na(\gamma_l^d)^{0.5}$ for n-alkanes (reference line). Another method uses the saturated vapour pressure (p^o) of the probes to obtain the reference line [35]. This method, although empirical in nature, presents the advantage over the Schultz & Lavielle method that the required p^o values of the probes are easily accessed from the literature whereas the a values of some probes are not available and/or are more uncertain (dependent on the orientation of the molecules on the material surface, e.g. 1-alkenes). The reference line may also be obtained by plotting the $RT\ln(V_n)$ vs. the number of carbon atoms.

$$\Delta G_a^s = -RT\ln\frac{V_n}{V_{n,ref}} \tag{6}$$

A nanomorphology index ($IM\chi_T$) has been proposed to assess the surface nanoroughness (Eq. (7)). Here, χ_T is the previously defined topological index of a branched alkane or cycloalkane (e.g. cyclohexane) [36] and χ_{exp} is the experimental value calculated for this topological index based on the measurement of the retention times of the non-linear alkane and the n-alkanes. Typically, the rougher is the surface the more negative is the $IM\chi_T$ value. On the contrary, for less rough surfaces, χ_{exp} approaches χ_T and $IM\chi_T$ tends to 0%.

$$IM\chi_T = 100\frac{(\chi_{exp} - \chi_T)}{\chi_T} \tag{7}$$

3. Results and discussion

3.1. Characterization of the clayey materials by powder X-ray diffraction and particle size analysis

The kaolinitic raw material and the metakaolinitic samples were previously analysed by XRD. For the raw material it was verified the presence of kaolinite and minor amounts of quartz. Muscovite and orthoclase (alkali feldspar) were also identified as accessory minerals. For the experimental metakaolins, the presence of kaolinite that has not been fully calcinated (metakaolinized) was still identified in the MK-750 sample. For the commercial metakaolin, the presence of anatase (TiO_2) and mullite as crystalline phases was also observed.

The particle size distribution (Table 1) of the kaolinitic raw material presented d_{50} = 1.5 μm, which results from the origin of the material, by opposition to the experimental metakaolinized materials that presented higher d_{50} values (between 8.3 μm and 3.5 μm) related with the aggregation promoted by the calcination process. As expected, the experimental metakaolinized samples showed lower d_{50} values after grinding (2.2 μm for MK-750-M and 2.5 μm for MK-940-M). The MK-USA showed a d_{50} similar to that of the kaolinitic raw material (Table 1). Finally, the obtained BET

Table 1
Physical parameters of the kaolinitic raw material and calcined kaolinitic clays.

	K	MK-750	MK-750-M	MK-840	MK-940	MK-940-M	MK-USA
d_{50} (μm)	1.5	8.3	2.2	7.7	3.5	2.5	1.8
BET ($m^2\ g^{-1}$)	19.0	16.3	16.5	9.8	9.7	13.1	17.9

Table 2
Surface chemical analysis (atomic percentage) by XPS of the kaolinitic raw material and calcined kaolinitic clays.

Element	K	MK-750	MK-750-M	MK-840	MK-940	MK-940-M	MK-USA
Si 2p	15.2	15.4	11.9	15.0	15.1	14.5	15.8
Al 2p	13.9	13.9	10.4	14.5	14.6	14.1	15.0
O 1s	66.9	60.7	65.0	62.2	61.6	62.6	62.7
C 1s	2.9	8.6	10.5	6.6	6.8	6.9	5.5
Mg 1s	0.1	0.1	0.2	0.5	0.2	nd	nd
K 2p	0.2	0.3	0.4	0.4	0.4	0.4	nd
Fe 2p1 + 2p3	0.1	0.4	0.6	0.1	0.5	0.7	nd
F 1s	nd	nd	nd	nd	0.2	nd	0.4
Ti 2p1 + 2p3	nd	nd	nd	nd	nd	nd	0.2
Si/Al	1.09	1.11	1.14	1.03	1.03	1.03	1.05

nd = not detected.

values, that measure the specific surface area, were within the range expected for metakaolinitic (and kaolinitic) materials and an increasing trend of the BET values with grinding as usual was observed (Table 1).

3.2. Characterization of the clayey materials by XPS

The XPS analysis (Table 2) of the clayey materials confirmed Si, Al and O as major elements mostly assigned to kaolinite or calcined kaolinite. In addition, minor amounts (<1%) of Mg, K, and Fe were generally found in the studied samples, related to the presence of contaminant minerals. MK-USA also showed a residual amount of Ti due to anatase identified in XRD and fluor was detected in two metakaolinitic materials. It should be noted that the surface contamination by adventitious carbon was also detected in all the samples. However, it was found that the Si/Al atomic ratio in all cases is very close to 1 (values between 1.03 and 1.14, Table 2), as expected for kaolinitic and metakaolinitic materials.

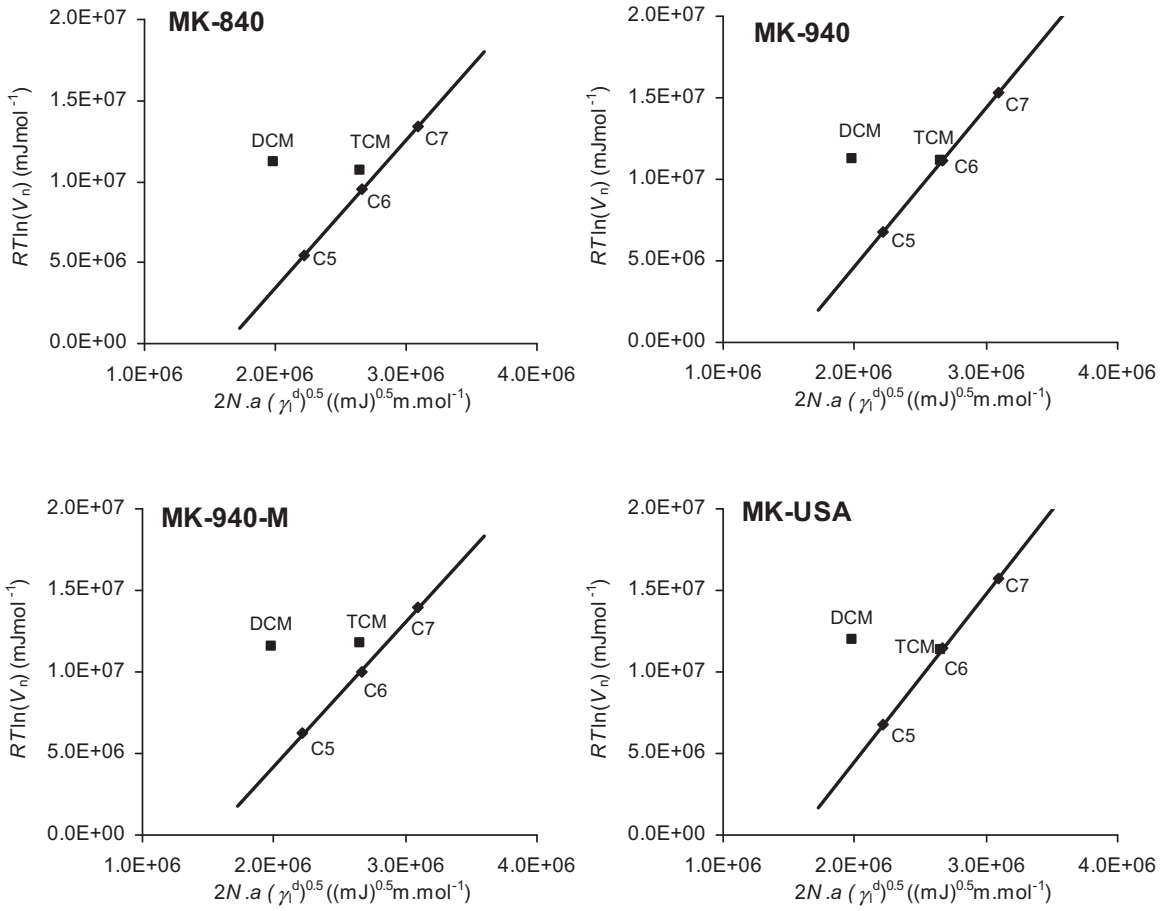

Fig. 1. Plots of $RT\ln(V_n)$ vs. $2Na(\gamma_l^d)^{0.5}$ used to calculate specific interaction parameters of TCM and DCM with several metakaolinitic samples.

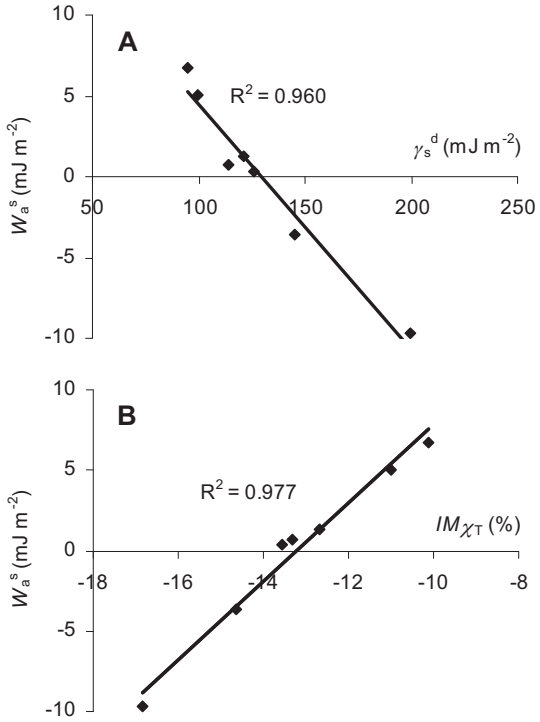

Fig. 2. Relations between the specific component of the work of adhesion (W_a^s) of TCM and the dispersive component of the surface free energy (γ_s^d) (A) or the nanomorphological index (IMχ_T) (B) for kaolinitic raw material and calcined kaolinitic materials.

3.3. Dispersive component of the surface free energy

The dispersive component of the surface free energy (γ_s^d) of the raw kaolinitic clay and the calcined kaolinitic clays was obtained by using the Dorris & Gray and the Schultz & Lavielle methods. The results are shown in Table 3. It is found that the values obtained by the Dorris & Gray approach are higher than those obtained using the Schultz & Lavielle approach but the relative difference between the results of the two methods is approximately the same for all samples studied, i.e., of ca. 20% (Table 3). This indicates that for metakaolinitic (and kaolinitic) materials the values determined for γ_s^d depend largely on the method chosen for their calculation but not the relative trends. In most of the reported IGC studies with clays the authors focused on using only the Dorris & Gray methodology to calculate γ_s^d and no comparison between the two methods was provided.

The γ_s^d was found to increase in the following order: MK-940-M < MK-840 < MK-940 < MK-750-M < MK-USA < MK-750 < K. The value determined for the kaolinitic raw material was in the range of other values reported in the literature [16,18]. For instance, values in the range of 156–212 mJ m^{-2} (at 100 °C and 120 °C) by the Dorris & Gray method were reported for several kaolinite samples whereas the value of 199.6 mJ m^{-2} was obtained in this work. With calcination the γ_s^d value decreased significantly from 200 mJ m^{-2} up to ca. 100 mJ m^{-2}. The decrease of γ_s^d with calcination has been previously mentioned [18]. It can be attributed mostly to the dehydroxylation process (loss of structural water) and to the collapse of the interlayer space of kaolinite structure, since both the hydroxyl groups and structural defects on the borders of the clay particles enhance the interaction with *n*-alkanes and consequently, the dispersive component of the surface free energy. Among the experimental calcined samples the one with the less extensive thermal degradation (MK-750) showed a higher γ_s^d value. This should reflect the fact that this sample still shows some kaolinite (higher γ_s^d) as proven by XRD. The commercial calcined sample showed a dispersive component of surface energy within the range of the three experimental calcined samples studied (126 mJ m^{-2} vs. 99–145 mJ m^{-2}), confirming a somewhat similar nature of all the calcined samples.

Interestingly, the γ_s^d value significantly diminished by grinding (milling) the calcined samples (16% for MK-750 and 17% for MK-940). With the grinding of the metakaolinitic samples and a consequent decrease of the particle size (Table 1), an increase of the overall surface energy could be expected. However, after grinding, the potential of the surface to undergo London dispersive interactions and/or Debye interactions was lower. XPS analysis revealed a slight increase of organic contaminants (C 1s content) on the surface of MK-750-M (Table 2). However, for MK-940-M and MK-940 the carbon content measured by XPS was similar and the differences in the γ_s^d value between these two samples were of the same range than those between MK-750-M and MK-750. Therefore, it is most probable that the variation of the γ_s^d with grinding can be attributed to a physical/morphological alteration of the metakaolinitic particles surface. Saada et al. [16] found for illites and kaolinites a correlation between the surface nanoroughness (measured by IGC from a morphological index obtained with branched alkane) and the dispersive component of the surface energy, that is, the clayey materials with higher surface nanorugosity had higher dispersive component of the surface energy. The authors suggested that the increasing structural surface defects on the borders of the clay particles (higher border nanoroughness) provided better insertion of the *n*-alkanes into the materials structure (higher interaction). Similar trend was also reported for talc impregnated with different ratios of polyethylene glycol [37]. In the present work, a nanomorphological index was calculated (Table 3) as well from the interaction measured with cyclohexane. It was found that this parameter increases with grinding and thus the decrease of the γ_s^d with grinding can be related to the production of a less rough surface. It should be noted that although metakaolinite presents a different structure from that shown by kaolinite, it inherits some degree of 1:1 layer structure of kaolinite [38], and thus the decreasing structural defects on the particles surface (lower border nanoroughness) of metakaolinite

Table 3
Dispersive component of the surface free energy (γ_s^d, mJ m^{-2}) and morphological index (IMχ_T) at 110 °C of the kaolinitic raw material and calcined kaolinitic clays.[a]

Material	γ_s^d (Schultz & Lavielle)	γ_s^d (Dorris & Gray)	Difference between methods[b]	IMχ_T
K	163	200	22%	−16.8
MK-750	121	145	20%	−14.6
MK-750-M	101	121	20%	−12.7
MK-840	83	99	20%	−11.0
MK-940	95	114	20%	−13.3
MK-940-M	78	94	20%	−10.1
MK-USA	105	126	20%	−13.6

[a] Coefficient of variation of $RT\ln(V_n)$ was lower than 1% for *n*-alkanes and cyclohexane.
[b] [γ_s^d (Dorris & Gray)−γ_s^d (Schultz & Lavielle)]/ γ_s^d (Schultz & Lavielle) × 100.

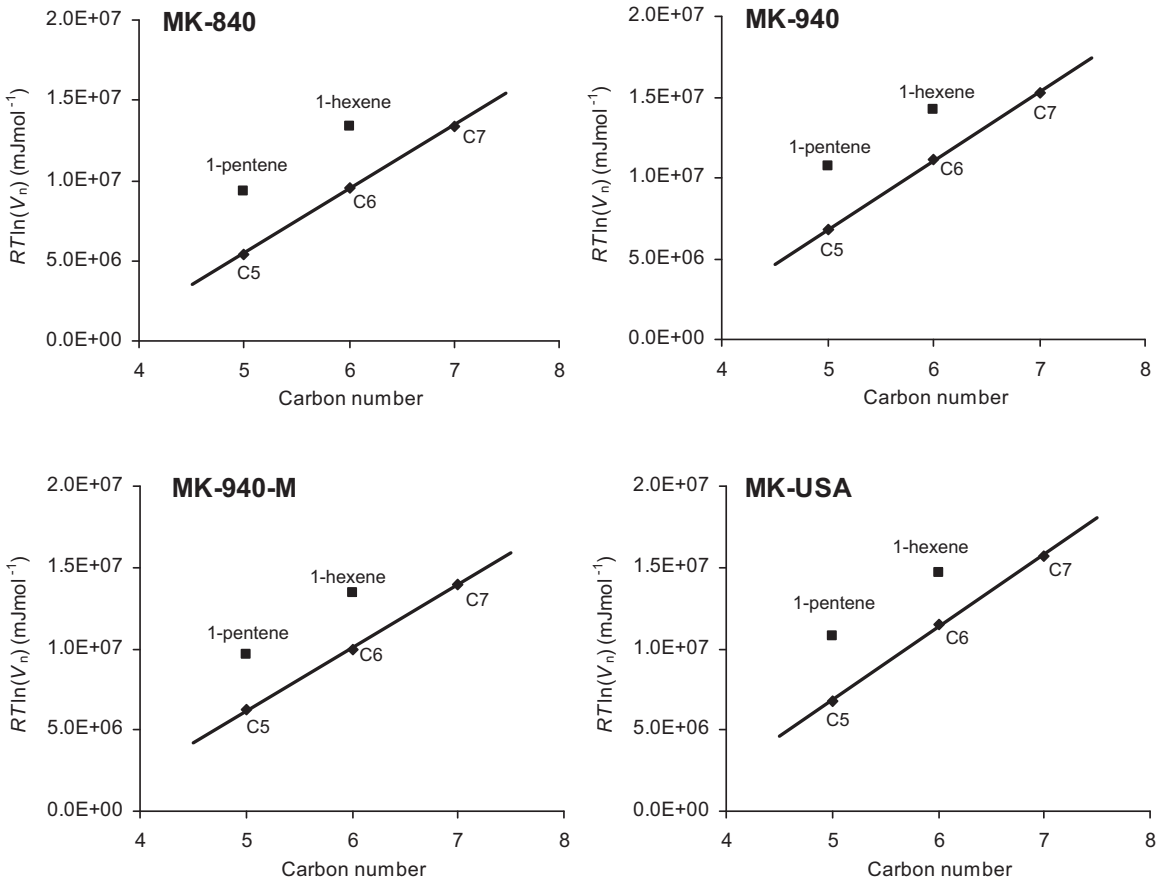

Fig. 3. Plots of $RT\ln(V_n)$ vs. carbon atoms number used to calculate specific interaction parameters of 1-pentene and 1-hexene on calcined kaolinitic materials.

will generate a lower interaction with the *n*-alkanes molecules. A decrease of γ_s^d with grinding has also been observed for attapulgite [25].

3.4. Specific interaction parameters obtained by IGC

Three different approaches were applied in the present work to calculate the specific component of the free energy of adsorption ($-\Delta G_a^s$) of the polar probes in the kaolinitic and metakaolinitic materials. Using Schultz & Lavielle approach only the $-\Delta G_a^s$ values of TCM and DCM could be obtained (since the required *a* values of the other measured polar probes are uncertain). The corresponding results of all the analysed samples are presented in Table 4 and a few representative graphical plots used to calculate the specific parameters are shown in Fig. 1.

For TCM, it was found that the $-\Delta G_a^s$ values are relatively small and, in some cases, namely for the initial clay and the MK-750 sample, even negative values were found (and, consequently, negative values for the work of adhesion) meaning that the interaction of this typical acidic probe with the samples' surface is not favoured. However, regarding DCM, much higher $-\Delta G_a^s$ values were always obtained (i.e., high values for W_a^s), as clearly shown in Fig. 1. Although TCM and DCM have similar electron acceptor properties, the fact that TCM is a bulkier probe than DCM should account for the more restricted specific interaction by steric reasons of the former with the surface of the clayey materials. Strong basic probes such as tetrahydrofurane or ethyl ether could not be measured because

Table 4
Specific component of the free energy of adsorption ($-\Delta G_a^s$, kJ mol^{-1}) and work of adhesion (W_a^s, mJ m^{-2}) at 110 °C of polar probes on the surface of the kaolinitic raw material and calcined kaolinitic clays.[a]

Material	(Schultz & Lavielle)				(Dorris & Gray)	
	TCM		DCM		1-pentene	1-hexene
	$-\Delta G_a^s$	W_a^s	$-\Delta G_a^s$	W_a^s	$-\Delta G_a^s$	$-\Delta G_a^s$
K	−2.58	−9.73	5.32	28.0	npd	npd
MK-750	−0.96	−3.62	5.80	30.6	3.42	npd
MK-750-M	0.34	1.27	7.80	41.1	3.49	2.97
MK-840	1.34	5.07	7.83	41.3	3.87	3.77
MK-940	0.20	0.74	6.77	35.7	3.96	3.10
MK-940-M	1.78	6.72	7.44	39.2	3.40	3.46
MK-USA	0.01	0.36	7.52	39.6	4.02	3.27

npd = not possible to determine.
[a] Coefficient of variation of $RT\ln(V_n)$ was lower than 2% for TCM, DCM and 1-alkenes.

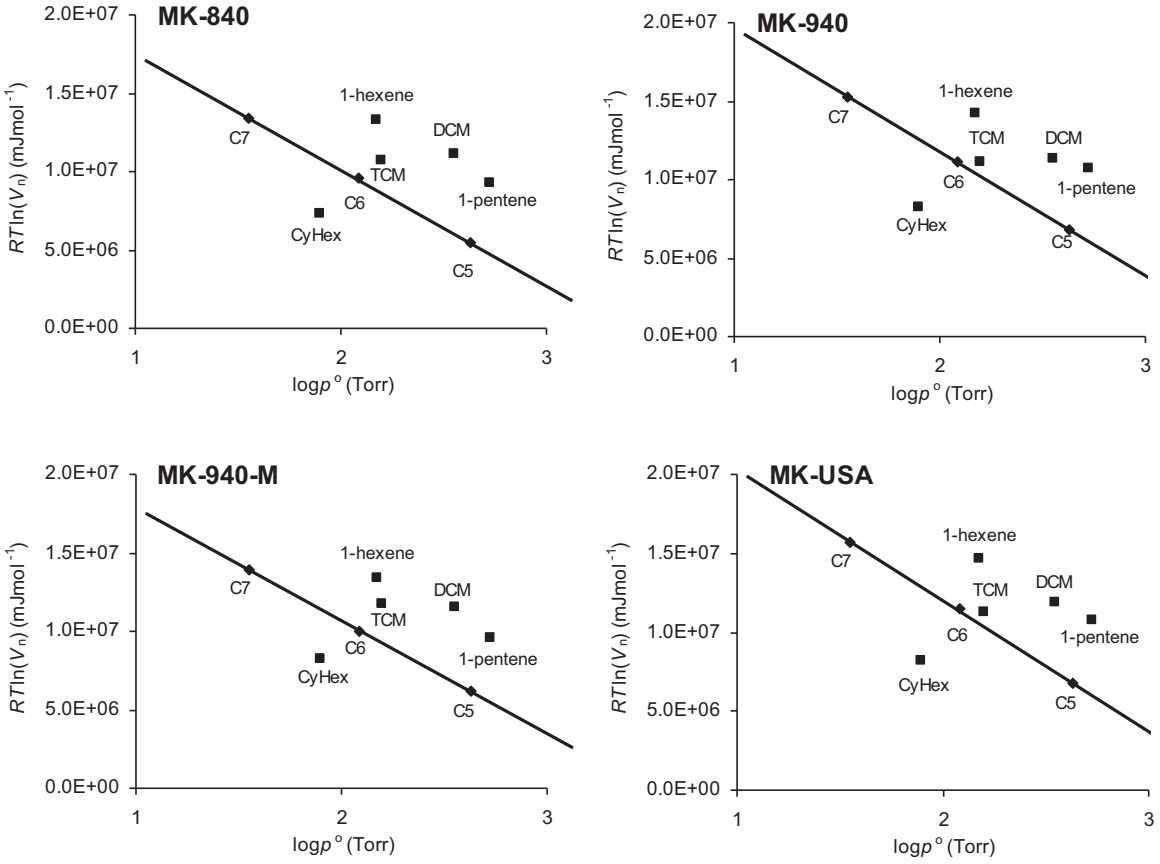

Fig. 4. Plots of $RT\ln(V_n)$ vs. saturated vapour pressure (p^o) of different probes in metakaolinitic samples.

they were retained too strongly in the materials. Overall, these results show the prevalence of the Lewis acidic character over the basic character of the materials surface.

In addition, it was found the $-\Delta G_a^s$(TCM) or W_a^s(TCM) varied approximately in the inverse order of the γ_s^d value (Fig. 2A), i.e., MK-940-M > MK-840 > MK-750-M > MK-940> MK-USA > MK-750 > K, but, on the other hand, no satisfactory correlation was obtained between the $-\Delta G_a^s$(DCM) and the γ_s^d value. The good fitting obtained between the specific interaction of TCM and the γ_s^d values may be largely related to changes in the surface nanoroughness of the materials, as confirmed by the plot shown in Fig. 2B. Metakaolinitic (and kaolinitic) surfaces with the lower nanoroughness will have the most energetic sites more accessible for interaction with the bulky TCM probe thus giving higher $-\Delta G_a^s$(TCM) value and also will provide a lower retention of the *n*-alkanes thus giving a lower γ_s^d.

With the less bulky probe, DCM, the polar (Lewis acid-base) interactions with the clayey materials predominate and the magnitude of the specific interaction with DCM (Table 4) may then be viewed as a relative measurement of the Lewis basicity of the surfaces. Thus, following Schultz and Lavielle approach, the calcined materials have higher specific interactions with DCM than the original material and, among the calcined samples that with some residual kaolinite (MK-750) also presented the lowest $-\Delta G_a^s$. Therefore, the thermal treatment of the kaolinitic clay promotes an apparent increase of the Lewis basic character of its surface. The condensation of acidic hydroxyl groups with the formation of new Al-O-Al linkages and changes in the co-ordination of aluminium from 6-fold to mainly 5- and 4-fold [38,39] in the calcined kaolinitic structure should be responsible for such effect on the surface properties.

With the grinding of the metakaolinitic materials (MK-750-M vs. MK-750 and MK-940-M vs. MK-940) the specific interaction with TCM increased (Table 4). Once more, this effect should be mainly due to a decrease of the surface nanoroughness of the metakaolinitic materials with grinding, as aforementioned, since a less rough surface allows a higher interaction with the bulky TCM. Apparently, the Lewis basicity ($-\Delta G_a^s$ of DCM) of the surface of the milled metakaolines was also slightly higher than that of the not milled. This could be one of the reasons, in addition to the reduction of particle size, why cationic exchange capacity typically increases by grinding this type of materials.

Since it was not possible to measure by IGC the interaction of the kaolinitic and metakaolinitic surfaces with strong Lewis bases, the retention volumes with weak bases, such as 1-pentene and 1-hexene were considered as an alternative to assess the Lewis acidic behaviour of the materials surfaces. By using the Dorris & Gray approach, the specific component of the free energy of adsorption of these alkenes (comparison with *n*-alkanes) on the materials surface was obtained (Fig. 3 and Table 4). All the values obtained for the correspondent specific interactions are positive confirming the significant interaction of the clayey surfaces with the π electron donor bases and thus its high degree of Lewis acidity. However, no definite conclusions could be drawn regarding the effect of the grinding on the metakaolines Lewis basic properties because the $-\Delta G_a^s$ values with 1-pentene or 1-hexene did not show a systematic trend with grinding.

Finally, the magnitude of the specific interactions of the measured polar probes with the studied clayey surfaces was calculated by the Flour and Papirer approach (Fig. 4 and Table 5). By this method, interactions of all probes can be compared and, in particular, interactions of weak bases can be compared with those of Lewis

Table 5
Values of specific interaction energies ($-\Delta G_a^s$, kJ mol^{-1}) at 110 °C assessed by the Flour & Papirer method for polar probes on the kaolinitic raw material and calcined kaolinitic clays.[a]

Material	TCM	DCM	1-Pentene	1-Hexene	Cyclohexane	1-Pentene/DCM ratio
K	−1.57	1.50	npd	npd	−6.96	npd
MK-750	−0.09	2.52	4.22	npd	−5.30	1.67
MK-750-M	1.14	4.80	4.24	3.81	−4.33	0.88
MK-840	2.07	5.11	4.55	4.54	−3.51	0.89
MK-940	0.97	3.86	4.72	3.85	−4.36	1.22
MK-940-M	2.49	4.79	4.14	4.03	−3.20	0.86
MK-USA	0.91	4.46	4.77	4.15	−4.65	1.07

npd = not possible to determine.
[a] Coefficient of variation of $RT\ln(V_n)$ was lower than 2% for all measured probes.

acids on the same basis. Among the polar probes, it was confirmed that TCM shows the lowest specific interaction with the materials surface due to the aforementioned steric constraint. In addition, following this approach, it was found that the specific interactions of the metakaolinitic surfaces with weak bases (1-pentene and 1-hexene) are of similar range of those with DCM because the $-\Delta G_a^s$(1-pentene)/ $-\Delta G_a^s$(DCM) ratio is close to 1 (Table 5), except in the case of MK-750 which presents a more acidic surface due to some amount of original clay. Moreover, this ratio seems to slightly decrease with the grinding of the metakaolinitic material showing again that the grinding process promotes a reduction of the prevalence of the acidic character over the basic character of the surface.

The specific interaction with cyclohexane (apolar) showed always a negative value due to steric hindrance in the adsorption process of this cyclic structure [27]. However, both the calcination of the kaolinitic raw material and the grinding of the metakaolinitic materials were found to favour this interaction (higher values for the $-\Delta G_a^s$ were found). As discussed, this is evidence that changes occurred in the surface nanomorphology during the thermal and physical treatments. Less rough surfaces at the nanoscale will provide higher interaction with the different geometric conformations of cyclohexane molecules.

4. Conclusions

Inverse gas chromatography, at infinite dilution, was found to be a valuable tool to differentiate the surface of metakaolinitic clays produced by calcination at different temperatures from a kaolinitic material and to assess the effect of grinding on the surface of metakaolinitic materials, which are topics of high relevance in the context of metakaolinitic materials processing. During calcination of kaolinitic to metakaolinitic material, it was found that, besides the reduction of the dispersive component of the surface energy, the Lewis basic properties of the material surface increased, as measured by the specific interaction with dichloromethane, which was attributed to the condensation of acidic hydroxyl groups with the formation of new Al-O-Al linkages in the metakaolinitic structure.

Interestingly, the grinding of the metakaolinitic materials afforded a decrease of the dispersive component of the surface energy and a higher interaction with bulky probes. These results were related to the production of a less rough surface of the metakaolinitic clay by grinding, as measured by the nanomorphology index of cyclohexane. An apparent increase of the Lewis basic properties of the surface also occurred with grinding. These conclusions could be of interest to understand the known behaviour of milled metakaolins vs. the not milled ones in terms of cation exchange capacity or pozzolanic activity. Further studies are in progress on this subject.

Acknowledgments

This research was supported by the Projecto Estratégico (PEst-OE/CTE/UI4035/2014) and Research Project "TACELO - Studies for the conservation of monumental terracotta sculptures from Alcobaça monastery" (PTDC/CTE-GIX/111825/2009) financed by the Fundação para a Ciência e a Tecnologia (FCT). The XPS analysis was accomplished in Centro de Materiais da Universidade do Porto (CEMUP).

References

[1] J. Bai, Fabrication and properties of porous mullite ceramics from calcined carbonaceous kaolin and α-Al_2O_3, Ceram. Int. 36 (2010) 673–678.
[2] P. He, D. Jia, Low-temperature sintered pollucite ceramic from geopolymer precursor using synthetic metakaolin, J. Mater. Sci. 48 (2013) 1812–1818.
[3] C. Kohl, R. Berube, Kaolin-based systems for increasing paper opacity, Wochenblatt fur Papierfabrikation 132 (2004) 1400–1405.
[4] J. Shen, Z. Song, X. Qian, W. Liu, Modification of papermaking grade fillers: a brief review, Bioresources 4 (2009) 1190–1209.
[5] M. Said-Mansour, E. Kadri, S. Kenai, M. Ghrici, R. Bennaceur, Influence of calcined kaolin on mortar properties, Constr. Build. Mater. 25 (2011) 2275–2282.
[6] M.S. Morsy, S.H. Alsayed, Y.A. Salloum, Development of eco-friendly binder using metakaolin-fly ash-lime-anhydrous gypsum, Constr. Build. Mater. 35 (2012) 772–777.
[7] A.K. Parande, A. Sivashanmugam, H. Beulah, N. Palaniswamy, Performance evaluation of low cost adsorbents in reduction of COD in sugar industrial effluent, J. Hazard. Mater. 168 (2009) 800–805.
[8] A.M. Rashad, Metakaolin as cementitious material: History, scours, production and composition—A comprehensive overview, Constr. Build. Mater. 41 (2013) 303–318.
[9] A.J.M. Lima, S. Iwakiri, M.G. Lomelí-Ramírez, Use the residue of Pinus spp, high reactivity metakaolin and residue of ceramic calcined in wood-cement composites, Madera Bosques 17 (2011) 47–65.
[10] S. Roopa, Siddaramaiah, Mechanical, thermal and morphological behaviors of castor oil based PU/PS interpenetrating polymer network-metakaolin composites, J. Macromol. Sci., Part A Pure Appl. Chem. 47 (2010) 689–696.
[11] S.R. Thimmaiah, Siddaramaiah, Investigation of carbon black and metakaolin cofillers content on mechanical and thermal behaviors of natural rubber compounds, J. Elastomers Plast. 45 (2013) 187–198.
[12] S. Kiat-Amnuay, M. Beerbower, J.M. Powers, R.D. Paravina, Influence of pigments and opacifiers on color stability of silicone maxillofacial elastomer, J. Dent. 37 (2009) e45–e50.
[13] A. Al-Harahsheh, M. Al-Harahsheh, A. Al-Otoom, M. Allawzi, Effect of demineralization of El-lajjun Jordanian oil shale on oil yield, Fuel Process. Technol. 90 (2009) 818–824.
[14] N.M. Ahmed, Comparative study on the role of kaolin, calcined kaolin and chemically treated kaolin in alkyd-based paints for protection of steel, Pigm. Resin Technol. 42 (2013) 3–14.
[15] Z. Yunsheng, S. Wei, L. Zongjin, Composition design and microstructural characterization of calcined kaolin-based geopolymer cement, Appl. Clay Sci. 47 (2010) 271–275.
[16] A. Saada, E. Papirer, H. Balard, B. Siffert, Determination of the surface properties of illites and kaolinites by inverse gas chromatography, J. Colloid Interface Sci. 175 (1995) 212–218.
[17] H. Balard, A. Saada, B. Siffert, E. Papirer, Influence of water on the retention of organic probes on clays studied by IGC, Clays Clay Miner. 45 (1997) 489–495.
[18] W.M. Burry, D.S. Keller, Effects of dehydration on the apolar surface energetics of inorganic paper fillers, J. Chrom. A 972 (2002) 241–251.
[19] V. Kovacecic, M. Leskovac, S.L. Blagojevic, Morphology and failure in nanocomposites. Part II: surface investigation, J. Adhes. Sci. Technol. 16 (2002) 1915–1929.

[20] G.J. Price, D.M. Ansari, An inverse gas chromatography study of calcination and surface modification of kaolinite clays, Phys. Chem. Chem. Phys. 5 (2003) 5552–5557.
[21] Y.C. Yang, P.R. Yoon, Examination of the surface properties of kaolinites by inverse gas chromatography: dispersive properties, Kor. J. Chem. Eng. 24 (2007) 165–169.
[22] N. El-Thaher, P. Choi, Effect of preheating treatment on the measurement heats of adsorption of organic probes on clays with different surface compositions, Ind. Eng. Chem. Res. 51 (2012) 7022–7027.
[23] T.J. Bandosz, J. Jagiello, K.A.G. Amankwah, J.A. Schwarz, Chemical and structural properties of clay minerals by inorganic and organic material, Clay Miner. 27 (1992) 435–444.
[24] A. Tamayo, J. Kyziol-Komosinska, M.J. Sánchez, P. Calejas, J. Rubio, M.F. Barba, Characterization and properties of treated smectites, J. Eur. Cer. Soc. 32 (2012) 2831–2841.
[25] L. Boudriche, B. Hamdi, Z. Kessaíssia, R. Calvet, A. Chamayou, J.A. Dodds, H. Balard, An assessment of the surface properties of milled attapulgite using inverse gas chromatography, Clays Clay Miner. 58 (2010) 143–153.
[26] L. Boudriche, R. Calvet, B. Hamdi, H. Balard, Surface properties evolution of attapulgite by IGC analysis as a function of thermal treatment, Colloids Surf. A 399 (2012) 1–10.
[27] D.M. Ansari, G.J. Price, Chromatographic estimation of filler surface energies and correlation with photodegradation of kaolin filled polyethylene, Polymer 45 (2004) 1823–1831.
[28] R.M.T. Sánchez, E.I. Basaldella, J.F. Marco, The effect of thermal and mechanical treatments on kaolinite: characterization by XPS and IEP measurements, J. Colloid Interface Sci. 215 (1999) 339–344.
[29] D.P. Kamdem, B. Riedl, Inverse gas chromatography of lignocellulosic fibers coated with a thermosetting polymer: use of peak maximum and conder and young methods, J. Colloid Interface Sci. 150 (1992) 507–516.
[30] P. Mukhopadhyay, H.P. Schreiber, Aspects of acid-base interactions and use of inverse gas chromatography, Colloids Surf. A 100 (1995) 47–71.
[31] J.M.R.C.A. Santos, J.T. Guthrie, Analysis of interactions in multicomponent polymeric systems: The key-role of inverse gas chromatography, Mater. Sci. Eng. R 50 (2005) 79–107.
[32] J.A.F. Gamelas, The surface properties of cellulose and lignocellulosic materials assessed by inverse gas chromatography: a review, Cellulose 20 (2013) 2675–2693.
[33] G.M. Dorris, D.G. Gray, Adsorption of *n*-alkanes at zero surface coverage on cellulose paper and wood fibres, J. Colloid Interface Sci. 77 (1980) 353–362.
[34] J. Schultz, L. Lavielle, C. Martin, The role of the interface in carbon fibre-epoxy composites, J. Adhesion 23 (1987) 45–60.
[35] C. Saint Flour, E. Papirer, Gas solid chromatography: a method of measuring surface free energy characteristics of short glass fibers. 2. Through retention volumes measured near zero surface coverage, Ind. Eng. Chem. Prod. Res. Dev. 21 (1982) 666–669.
[36] E. Brendlé, E. Papirer, A new topological index for molecular probes used in inverse gas chromatography for the surface nanorugosity evaluation, J. Colloid Interface Sci. 194 (1997) 207–216.
[37] M. Comard, R. Calvet, J.A. Dodds, H. Balard, Coupling of inverse gas chromatography at infinite dilution (IGC-ID) with a controlled modification of a solid surface, J. Chrom. A 969 (2002) 93–96.
[38] S. Sperinck, P. Raiteri, N. Marks, K. Wright, Dehydroxylation of kaolinite to metakaolin- a molecular dynamics study, J. Mater. Chem. 21 (2011) 2118–2125.
[39] C.E. White, L.M. Perander, J.L. Provis, J.S.J. van Deventer, The use of XANES to clarify issues related to bonding environments in metakaolin: a discussion of the paper S. Sperinck et al., "Dehydroxylation of kaolinite to metakaolin - a molecular dynamics study", J. Mater. Chem., 2011, 21, 2118–2125, J. Mater. Chem. 21 (2011) 7007–7010.